

Supplementary Materials

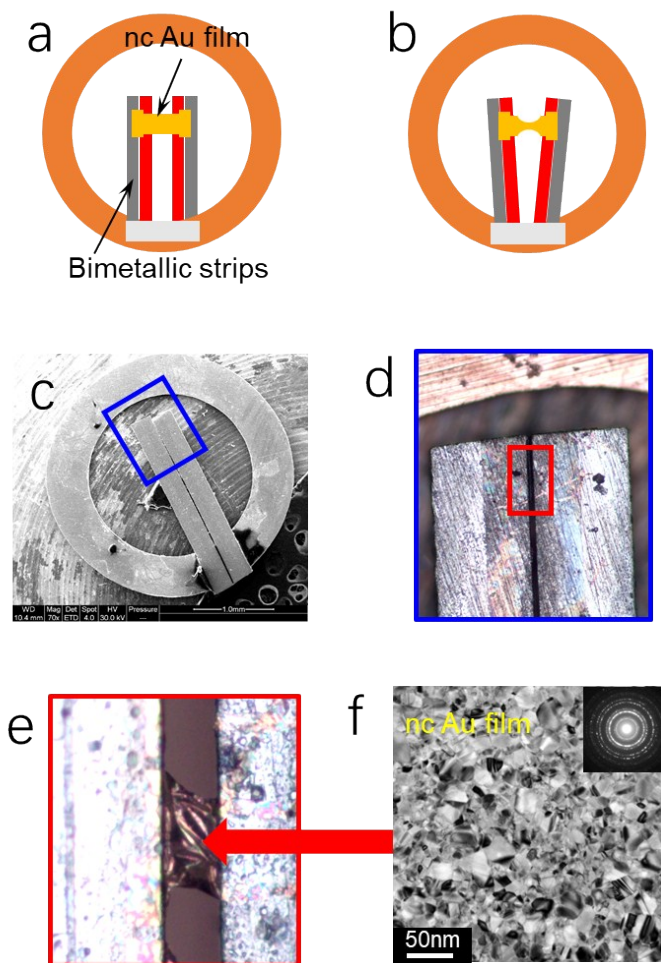


Figure S1. (a, b) Schematic of the TEM bimetallic strain actuator before and after deformation. (c) Low magnification observation of the home-made TEM bimetallic strain actuator. (d) Enlarged image from the blue frame in **c** exhibits the morphology of the bimetallic strips. (e) A nanocrystalline (nc) Au film was fixed on the bimetallic strips. The central part is electron beam transparent. (f) The nc Au film thickness of ~ 50 nm consists of nanosized and columnar grains. The insertion indicates the selected electron diffraction pattern.

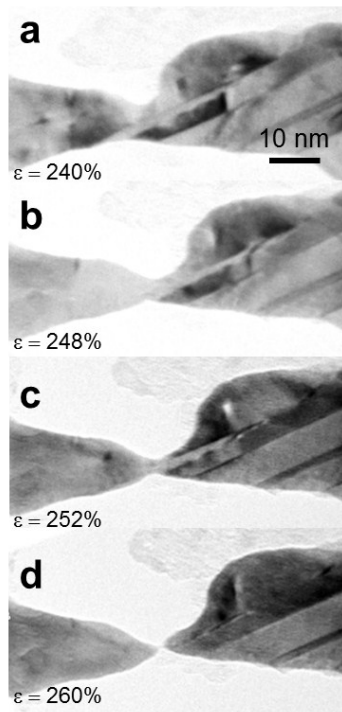


Figure S2 With further pulling, the eventual elongation of the nanowire reached to $\sim 260\%$ before fracture.

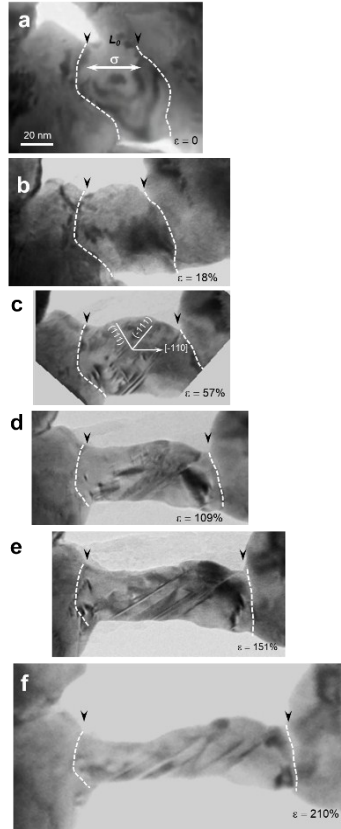


Figure S3. The low magnification TEM images exhibit the deformation of the Au nanowire with strain in the range of 0 - 210%, as well as the morphology changes of surrounding nanocracks.

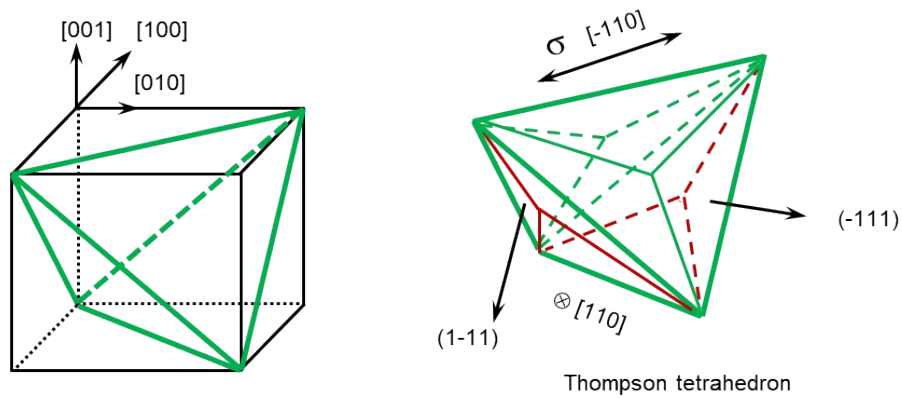


Figure S4 Thompson tetrahedron in a 3-dimensional model shows the 12 $\{111\}\langle 110\rangle$ slip systems.

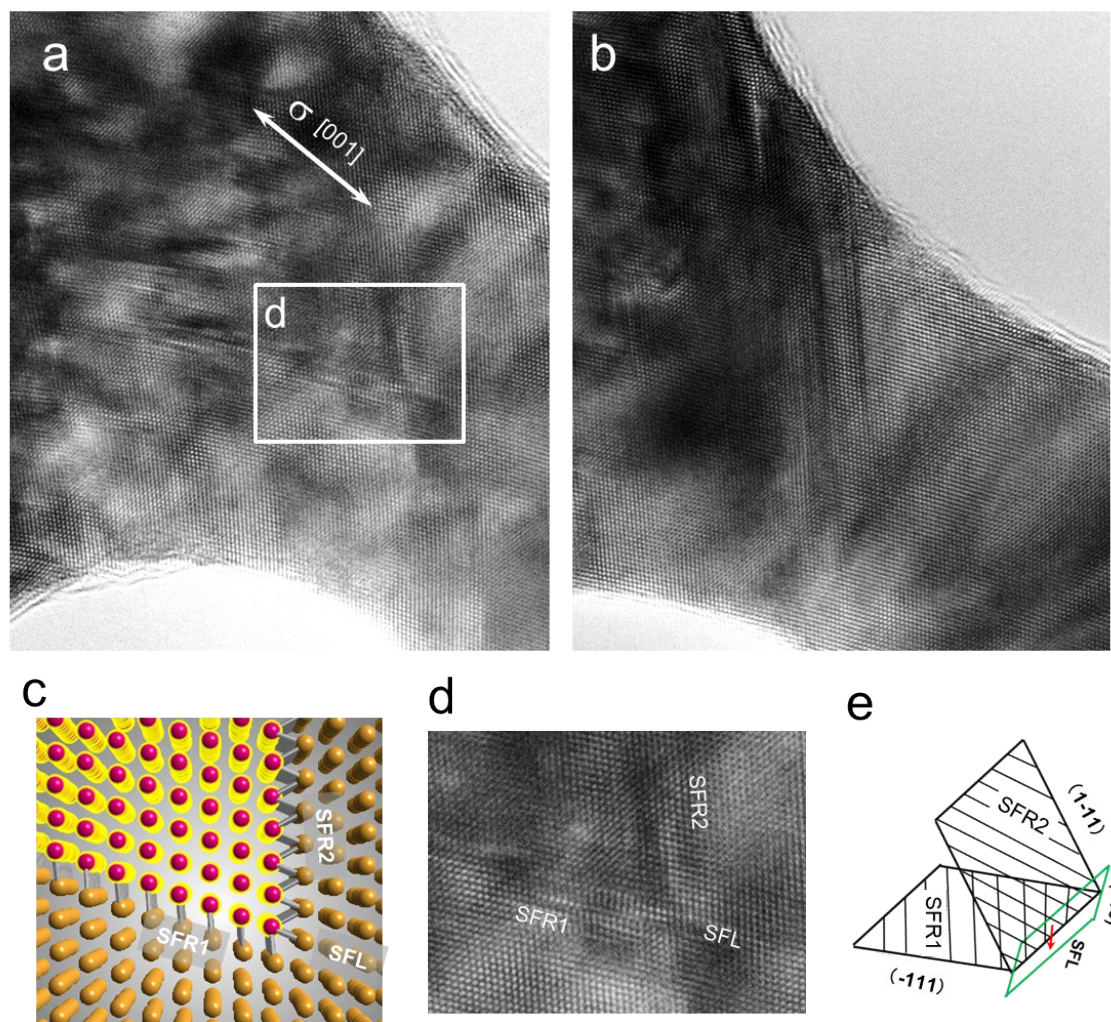


Figure S5 In situ atomic scale observations of the plastic deformation process of another Au nanowire with the starting size of ~ 37 nm. (a) A few SFRs with widths between 5-10 nm emitted from free surface and the left GB. The continuous dislocation nucleation, motion and annihilation took place in very few surface dislocation sources, resulting in the local strain and rapid necking. In this context, plastic strain with $\sim 40\%$ uniform elongation and $\sim 120\%$ total strain before fracture was observed. (b) The partial behaviors was dominant with the feature size reduced to ~ 28 nm. (c, e) The atomic model of a typical SFR. (d) The enlarged atomic image extracted from (a) exhibits the atomic configuration of a typical SFR.

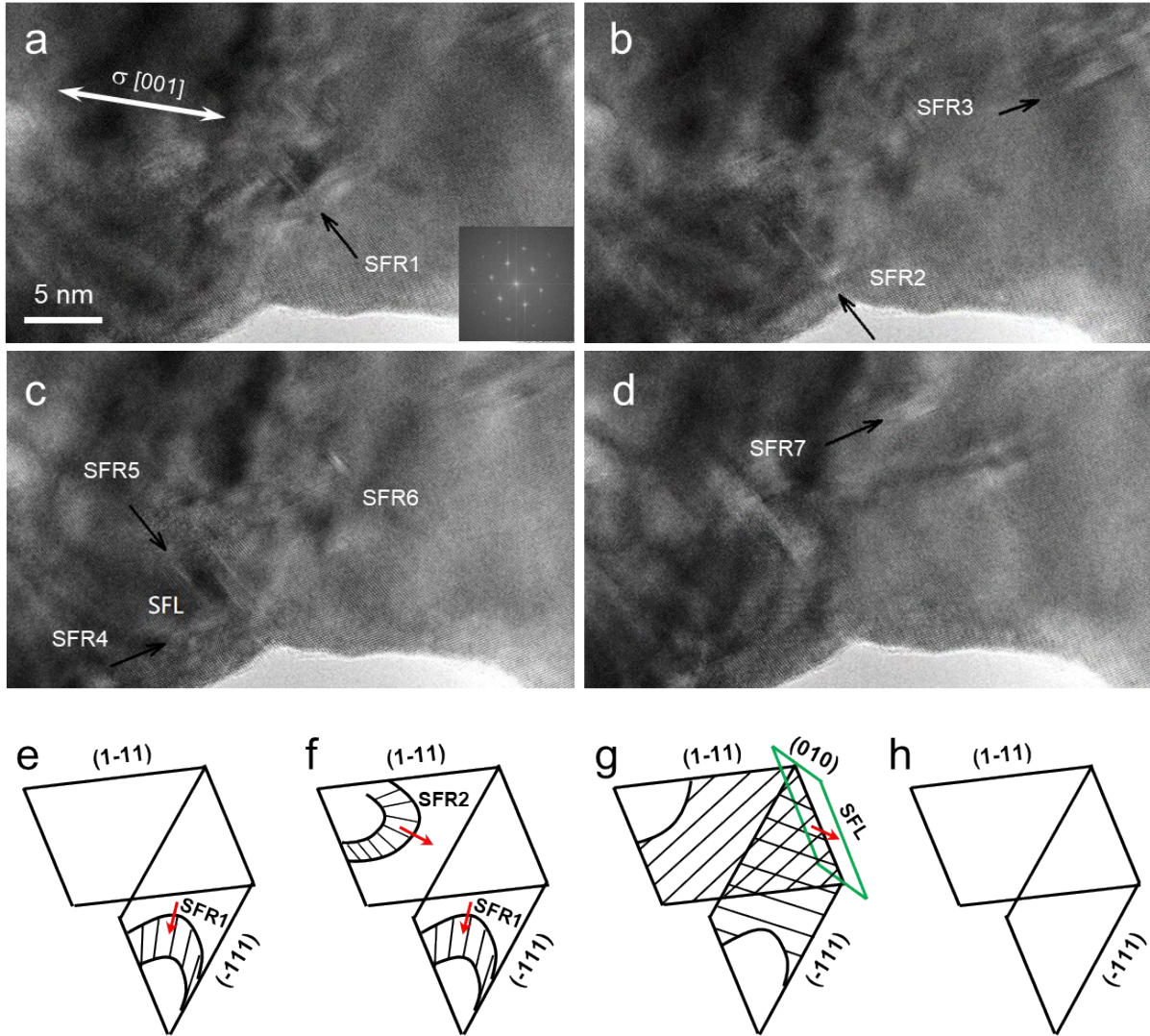


Figure S6 In situ atomic scale observations of the motion of SFRs in another Au nanowire with the starting size of ~ 45 nm. (a-d) The SFRs nucleated, moved and escaped on different glide planes of $(1\bar{1}1)$ and $(11\bar{1})$. Dislocation reactions were captured during the slip of SFRs in (c). Two partial dislocations formed a stacking fault lock (SFL). The Burgers vector of SFL was calculated to be $1/6[101]a$. This SFL was unlocked with further straining.

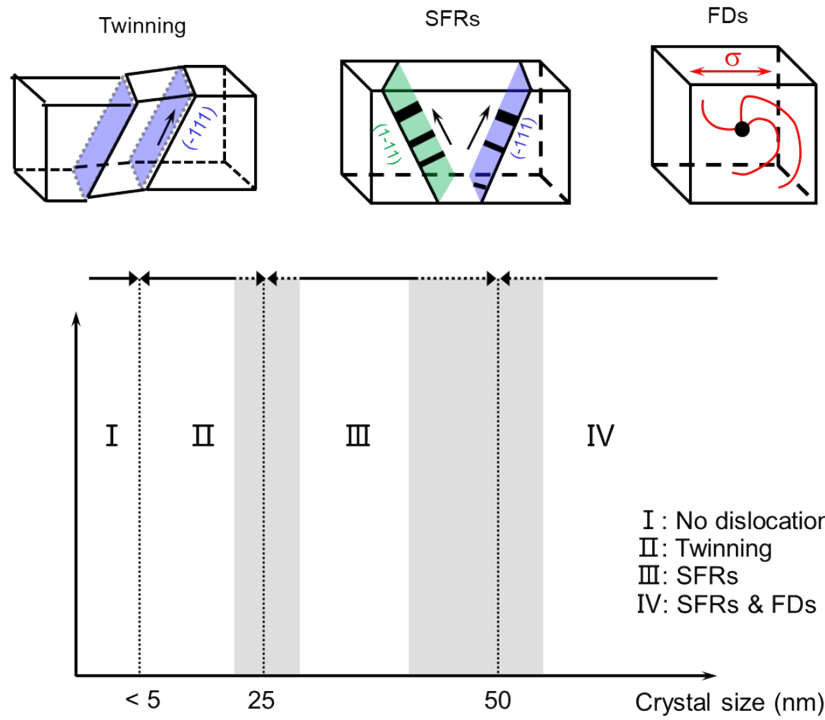


Figure S7 The schematic illustrates the SFRs and deformation twins dominated the plastic deformation at different deformation stages. Before formation of deformation twins, the FDs can be dissociated into different width of SFRs with feature size reduction.

σ along $\langle 110 \rangle$							σ Along $\langle 110 \rangle$ + rotate 10°						
Slip plane	(1-11)			(-111)			Slip plane	(1-11)			(-111)		
Glide direction	[-110]	[-101]	[01-1]	[110]	[101]	[0-11]	[-110]	[-101]	[01-1]	[110]	[101]	[0-11]	
Schmidt factor	0.41	0.41	0	0.41	0.41	0	0.30	0.30	0	0.44	0.44	0	

Slip plane	(1-11)			(-111)			Slip plane	(1-11)			(-111)		
Glide direction	[-112]	[121]	[21-1]	[1-12]	[-1-21]	[211]	[-112]	[121]	[21-1]	[1-12]	[-1-21]	[211]	
Schmidt factor	0.24	0.24	0.47	0.24	0.24	0.47	0.16	0.16	0.36	0.25	0.25	0.49	

Table S1.